Journal of Catalysis **200,** 160–170 (2001)
doi:10.1006/jcat.2001.3195, available online at http://www.idealibrary.com on IDEAL®

Catalytic Activity of Cu-Beta Zeolite in NO Decomposition: Effect of Copper and Aluminium Distribution

Jiří Dědeček, Oleg Bortnovsky,[1] Alena Vondrová, and Blanka Wichterlová

J. Heyrovský Institute of Physical Chemistry, Academy of Sciences of the Czech Republic, Dolejškova 3, CZ-182 23 Prague 8, Czech Republic

Received November 27, 2000; revised January 31, 2001; accepted February 2, 2001; published online April 18, 2001

Catalytic activity in NO decomposition of Cu-Beta zeolites with different Cu/Al/Si composition, diffuse reflectance UV–vis–NIR spectra of Cu ions of hydrated Cu-Beta zeolites, and concentration of Brønsted and Lewis sites in parent Beta zeolites, determined by quantitative analysis of FTIR spectra of adsorbed d_3-acetonitrile, were investigated. Cu-Beta zeolites exhibit high and stable activity in NO decomposition in the temperature range 580–750 K and Si/Al ratio 12.7–42. Strong dependence of activity in NO decomposition per Cu ion (TOF) on Cu/Al loading indicates the presence of three Cu species in Cu-Beta zeolites. Cu ions incorporated at low Cu loading are balanced by two framework Al atoms and are inactive in NO decomposition. Species responsible for NO decomposition are formed at medium Cu loading and represent Cu ions balanced by single-framework Al atoms. At high Cu loading, a new type of inactive, noncationic Cu species (small clusters of Cu_2O) is formed. Brønsted and Lewis sites themselves do not contribute to the catalytic activity of Cu-Beta zeolites in NO decomposition. However, the presence of Lewis sites in the parent zeolites is connected with the occurrence of the framework sites containing two close Al atoms and bonding the Cu ions which are not active in NO decomposition. A comparison of Cu ion activity in Beta and ZSM-5 is discussed.

Key Words: **NO decomposition; copper; Beta zeolite; Cu-Beta; Cu-zeolite; aluminium distribution.**

INTRODUCTION

High activity of the Cu ions exchanged in the ZSM-5 zeolite in NO decomposition is well known (1, 2). Besides that catalyst, we reported a comparable activity for the Cu ions, in terms of turn-over frequency (TOF), exchanged in MeAlPO-5 and -11. The Cu ions active in NO decomposition in both these matrices were suggested to be balanced by a low local negative framework charge, i.e., by a single Al atom; such a Cu ion environment supports the existence of monovalent copper, a valence state active in NO decomposition. Despite the fact that the Cu ions exchanged in molecular sieves do not satisfy as catalysts the required parameters for industrial application of NO decomposition, there is current interest in analyzing the structure and properties of these unique active Cu sites. The nature of the reaction center is still under discussion. Single Cu^+ ions, two neighboring Cu^+, adjacent Cu^+ and O centers, bridged Cu^{2+}–O–Cu^{2+} structures, and Cu^{2+}–O^- species have been suggested as the active sites in NO decomposition (3–26).

We have shown (15–18) that the Cu site in ZSM-5 active in NO decomposition is easily reduced, possesses a low positive charge on the divalent Cu cation, and exhibits open, close to planar, coordination. This Cu site has been suggested to be adjacent to a single Al framework atom. A comparison of the MeAlPOs and MFI framework topology indicates that the active Cu species might be formed in matrices with different framework structures and at different cationic sites (27–29).

This contribution describes the activity of the Cu ions implanted in Beta zeolites in NO decomposition. The effect of Cu/Al/Si composition, the presence of H^+ and Na^+ ions and Al-Lewis sites in the parent zeolites, and the structure of the Cu ions on their activity is analyzed. The results show that the Cu-Beta zeolites with different distributions of framework Al atoms provide more general insight into the structure of the Cu ions active and, on the other hand, inactive in NO decomposition. The Cu ions balanced by close frameworks of Al atoms have been found to be inactive, while those in the vicinity of one Al atom exhibit the highest activity.

EXPERIMENTAL

Synthesis and Preparation of Parent Beta Zeolites

To investigate the effect of Si/Al composition on the catalytic activity of Cu-Beta zeolites, the zeolites with Si/Al = 12.7–42 were synthesized according to the modified procedures of Rubin *et al.* (30) and Eapen *et al.* (31) with tetraehylammonium hydroxide and bromide, respectively, as templates. The as-synthesized zeolites were calcined in a stream of dry nitrogen at 723 K for 12 h followed by calcination in dry oxygen at 773 K for 12 h to obtain

[1] On leave from the Research Institute of Inorganic Chemistry, Inc., Unipetrol, Ústí n/L.

0021-9517/01 $35.00

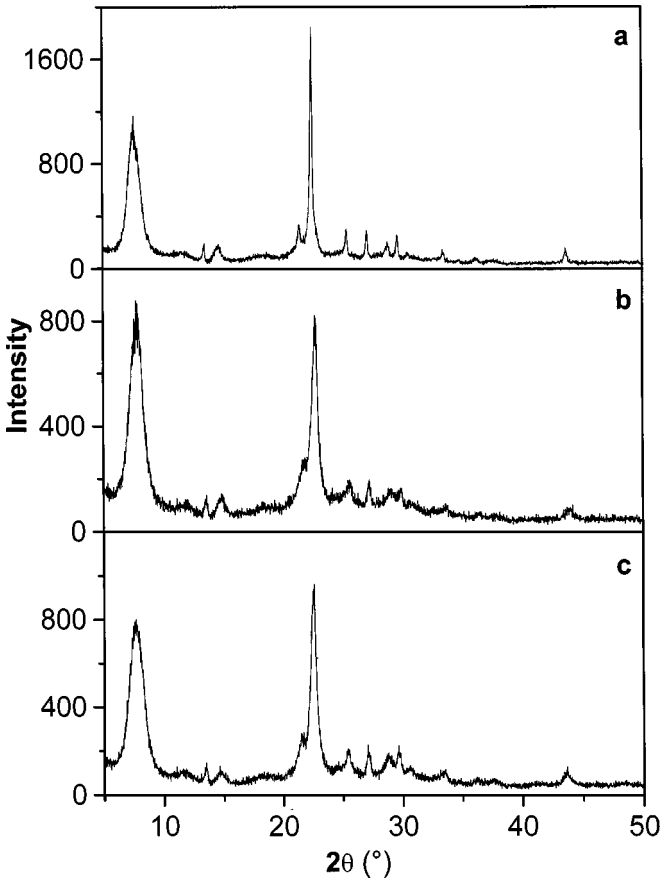

FIG. 1. X-ray diffraction patterns of Beta zeolites. (a) Na-Beta, Si/Al 42, (b) NH_4-beta, Si/Al 18.1, (c) H-Beta, Si/Al 14.3.

HNa-Beta. The crystallinity and phase purity of all the as-synthesized and calcined zeolites were good and related to the ICDD patern. This was checked by X-ray powder diffraction (Siemens D5005 diffractometer in the Bragg-Brentano geometry arrangement, using Cu$K\alpha$ radiation with a graphite monochromator and scintillation detector). Examples of the XRD patterns of calcined Beta zeolites are depicted in Fig. 1. The size of crystallites determined by scanning electron microscopy ranged from 0.1 to 0.5 μm.

Na-Beta zeolites were obtained by ion exchange of HNa-Beta with NaCl solution. Three times repeated exchange was carried out with 200 ml of 0.5 M NaCl per 1 g of a zeolite at room temperature (RT) for 24 h. NH_4-Beta zeolite was received by four times ion exchange of HNa-Beta with 100 ml of 0.5 M NH_4NO_3 per 1 g of a zeolite at RT for 4 h. H-Beta was prepared by deammination of NH_4-Beta in a nitrogen flow at 500°C for 6 h.

Cu Ion Exchange

Cu-Beta zeolites with Cu concentration ranging from 0.38 to 5.72 wt% were prepared by the ion exchange of Na-, NH_4-, and H-Beta zeolites with copper acetate at RT. The solids were washed with distilled water, filtered, and dried at RT. Chemical composition of Cu zeolites was determined by atomic absorption spectrometry after their dissolution. The results are given, together with the details on the ion exchange procedures, in Table 1.

Spectroscopy

Diffuse-reflectance (DR) vis–NIR spectra of hydrated, as-received Cu zeolites were obtained by using a Perkin–Elmer Lambda 19 spectrometer equipped with a diffuse reflectance attachment with an integrating sphere coated with $BaSO_4$. As a reference $BaSO_4$ was used as well. The spectra of the zeolites, placed in 5 mm-thick silica cells, were recorded with a scanning step of 1 nm and a slit width of 5 nm. The absorption intensities $F(R_\infty)$ were calculated using the Schuster–Kubelka–Munk theory (32).

FTIR spectra of dehydrated H-Beta zeolites and those after adsorption of d_3-acetonitrile (10 Torr) and short evacuation (15 min) at RT were recorded on transparent zeolite plates of ca. 10 mg cm^{-2} thickness, using a procedure given in Ref. (33). A Nicolet Magna-550 FTIR spectrometer was used with a KBr detector and a cell with CaF_2 windows connected to a vacuum apparatus and dosing system for acetonitrile. Spectra were recorded at RT with resolution of 2 cm^{-1} by collecting 200 scans for a single spectrum. The band intensities were normalized on the sample thickness of 10 mg cm^{-2}. The band at 2297 cm^{-1} corresponded to the interaction of the C≡N group with the acidic Brønsted site, while the bands at 2325–2330 and 2315 cm^{-1} reflected interaction of C≡N group with the strong and weak Lewis sites, respectively. By using the integrated intensity of the bands and corresponding extinction coefficients taken from Ref. 33, the concentration of Brønsted and Lewis sites was determined.

Catalytic Tests

The reaction was carried out at a downflow glass microreactor in the temperature range 500–800 K with a feed composition of 4000 ppm of NO in helium at a total flow of 100 ml/min and a catalyst weight of 400 mg. Prior to the reaction the catalyst was activated in a helium or oxygen stream or in NO (4000 ppm) with helium with a temperature increase of 5 K/min up to 720 K, held for 1 h, and cooled to the reaction temperature. NO decomposition was then measured at temperatures increasing in steps of 30 K. To achieve the temperature of the next measurement, the catalyst was heated in a NO/helium stream with an increase of 5 K/min. After the required temperature was reached, NO conversion was stabilized in 10–20 min. NO and NO_2 were analyzed with an accuracy of 0.5% at the inlet and outlet of the reactor with a Vamet 138 chemiluminescence analyzer (Czech Republic). In all experiments a very low

TABLE 1

Chemical Composition of Cu-Beta Samples and Conditions of Cu Ion Incorporation

Sample	Si/Al	Cu/Al	Cu acetate (mol/L)	Solution/ zeolite (mL/g)	Time of exchange (h)	Acid site in parent zeolite	
						Brønsted (mmol/g)	Lewis (mmol/g)
CuNa-Beta	12.7	0.61	0.05	40	3		
CuNa-Beta	12.7	0.63	0.05	50	4		
CuNa-Beta	12.7	0.57	0.05	40	4		
H-Beta	14.3	—	—	—	—	0.33	0.34
CuH-Beta	14.3	0.19	0.01	20	5		
CuH-Beta	14.3	0.31	0.015	30	5		
CuH-Beta[a]	14.3	0.87	0.05	120	12		
CuH-Beta[b]	14.3	0.99	0.05	120	6		
			0.05	120	24		
			0.1	90	24		
NH_4-Beta	16.9	—	—	—	—	0.61	0.15
CuNH_4-Beta	16.9	0.16	0.008	20	3		
CuNH_4-Beta	16.9	0.35	0.03	33	3		
CuNH_4-Beta	16.9	0.56	0.05	25	3		
Na-Beta	18.1	—	—	—	—	0.06	0.03
CuNa-Beta	18.1	0.22	0.013	15	3		
CuNa-Beta	18.1	0.50	0.014	50	4		
CuNa-Beta	18.1	0.61	0.05	30	3		
CuNa-Beta	18.1	0.66	0.05	35	3		
CuNa-Beta	18.1	0.69	0.05	40	3		
CuNa-Beta	18.1	0.69	0.024	50	4		
CuNa-Beta[a]	18.1	0.78	0.05	40	3		
CuNa-Beta[a]	18.1	0.88	0.05	35	3		
CuNa-Beta[a]	18.1	0.89	0.05	20	12		
CuNa-Beta[a]	18.1	0.90	0.05	30	3		
CuNa-Beta[a]	18.1	1.27	0.1	30	12		
NH_4-Beta	20.0	—	—	—	—	0.51	0.15
CuNH_4-Beta	20.0	0.28	0.015	15	4		
CuNH_4-Beta	20.0	0.37	0.015	30	12		
CuNH_4-Beta	20.0	0.60	0.025	50	12		
CuNH_4-Beta[a]	20.0	1.50	0.1	70	12		
CuNa-Beta	42.0	0.17	0.001	25	4		
CuNa-Beta	42.0	0.93	0.05	40	3		
CuNa-Beta[a]	42.0	2.15	0.05	40	12		
CuNa-Beta	42.0	1.17	0.05	30	3		
CuNa-Beta[a]	42.0	1.74	0.05	30	3		

[a] Twice ion exchange at the same condition.
[b] Three-step ion exchange.

concentration of NO_2 was detected in the products (<40 ppm). Only traces of N_2O (<5 ppm) were observed in the products by mass spectrometry (Hewlett Packard, 5971A).

RESULTS

Parent Beta Zeolites

In contrast to H-ZSM-5 zeolites, it is well known that H-Beta zeolites contain, besides the protonic Brønsted sites, a substantial concentration of Lewis sites (34, 35). FTIR spectra in the region of OH groups of parent H-, NH_4-, and Na-Beta zeolites after evacuation at 720 K, used in this study, are given in Fig. 2. Figure 3 depicts FTIR spectra of these zeolites after adsorption of d_3-acetonitrile. It is clearly seen that some of the bridging Si–OH–Al groups interact via hydrogen bonding, as reflected in a broad band ranging from 3700 up to ca. 3300 cm^{-1} and a lower intensity of the band at 3610 cm^{-1} (characteristic for unperturbed Si–OH–Al groups) than would correspond to the concentration of acidic Brønsted sites, as determined from adsorbed d_3-acetonitrile (Fig. 3; for details see Ref. 36). The concentration of acidic Brønsted sites was calculated from the band intensity at 2297 cm^{-1} and the concentrations of two types of Lewis sites were obtained from the intensities of the bands

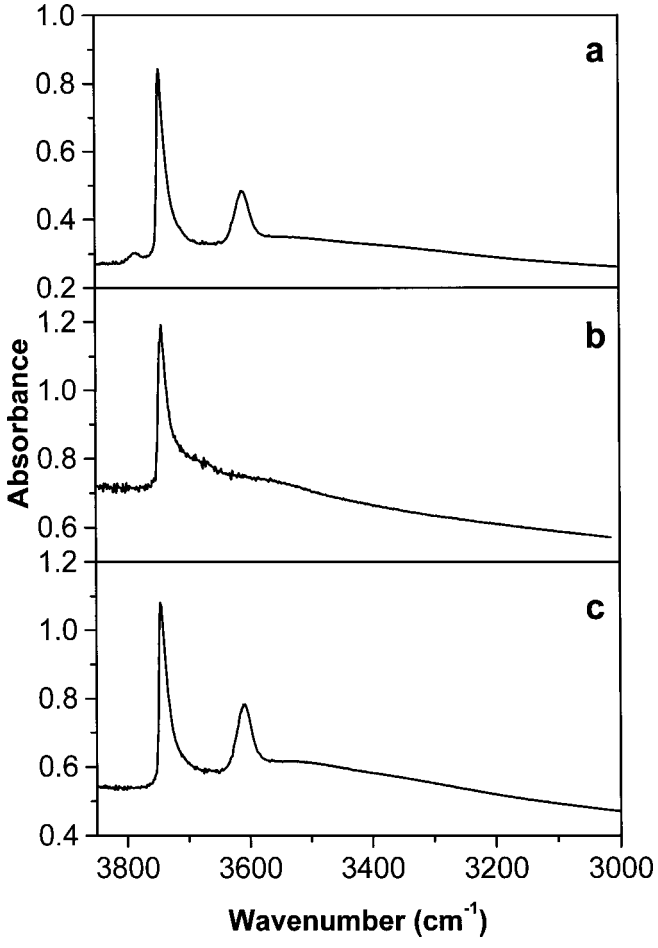

FIG. 2. FTIR spectra of parent Beta zeolites after evacuation at 720 K in the region of OH groups. (a) H-Beta Si/Al = 14.3, (b) Na-Beta Si/Al = 18.1, (c) NH_4-Beta Si/Al = 16.9.

at 2325 and 2315 cm^{-1}. The concentration of Brønsted sites and a sum of the concentrations of the two types of Lewis sites are given in Table 1.

These results evidenced a significant concentration of Al-Lewis sites together with the Si–OH–Al groups in the parent H-Beta zeolites. Some of these OH groups strongly interacted via hydrogen bonding. The Lewis sites were formed under deammination of NH_4 forms at heating conditions or template removal by calcination resulting directly in the H-Beta zeolite. The Na-Beta zeolites did not contain Lewis sites (see Fig. 3), which indicated that all (>97%) aluminum was located in the framework positions and no extraframework aluminum was present.

Cu Ion Exchange of Beta Zeolites

Cu ion exchange of H-, NH_4-, and Na-Beta zeolites carried out with Cu acetate solutions (see Table 1) led to high Cu ion exchange degrees exceeding the stoichiometric ratio for a divalent cation exchange, i.e., Cu/Al atomic ratio >0.5. Under the same conditions of Cu ion exchange performed by us with ZSM-5 (16), the exchange degrees obtained for ZSM-5 with different Si/Al ratios were much lower and usually reached maximum Cu/Al values up to 0.6. It is to be noted that after the Cu ion exchange of H- and NH_4-Beta zeolites a vast number of the Al centers exhibiting Lewis properties in the parent zeolites was transformed into the "regular" tetrahedral framework configuration (cf. Refs. 34 and 36).

As-received Cu-Beta zeolites prepared by ion exchange exhibited a blue color, originated from a broad absorption band with a maximum between 12,000 and 13,500 cm^{-1}, typical for the octahedral or bipyramidal complexes of Cu^{2+} ions with six water molecules (17). Normalized DR vis–NIR spectra of Cu-Beta zeolites are shown in Fig. 4. A sharp band at 7100 cm^{-1} corresponds to the combination vibration band (2ν) of OH band of water molecule. Shifts in the maximum and in the high energy edge of the broad Cu^{2+} band to higher wavenumbers of the Cu^{2+} indicates the

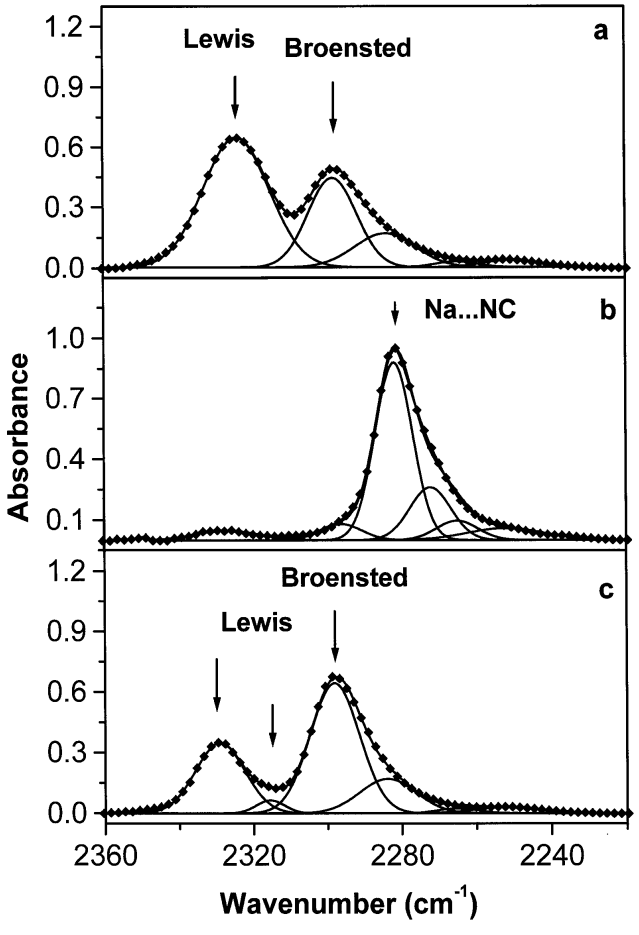

FIG. 3. FTIR spectra of parent Beta zeolites after d_3-acetonitrile adsorption and followed evacuation at RT in the region of C≡N group vibration. (a) H-Beta Si/Al = 14.3, (b) Na-Beta Si/Al = 18.1, (c) NH_4-Beta Si/Al = 16.9.

TABLE 2

Catalytic Activity of Cu-Beta Zeolite in NO Decomposition

Sample	Si/Al	Cu/Al	Cu (wt.%)	NO conversion (%)	TOF × 10^{-4} (s^{-1})
CuNa-Beta	12.7	0.61	3.28	12.7	2.9
CuNa-Beta	12.7	0.63	4.11	11.5	2.1
CuNa-Beta	12.7	0.57	3.52	9.2	2.0
CuH-Beta	14.3	0.19	1.12	0.4	0.3
CuH-Beta	14.3	0.31	1.82	3.5	1.4
CuH-Beta	14.3	0.87	4.94	23.0	3.5
CuH-Beta	14.3	0.99	5.54	21.0	2.8
$CuNH_4$-Beta	16.9	0.16	0.67	4.3	4.8
$CuNH_4$-Beta	16.9	0.35	1.53	8.9	4.4
$CuNH_4$-Beta	16.9	0.56	2.42	15.1	4.7
CuNa-Beta	18.1	0.22	0.91	0.0	0.0
CuNa-Beta	18.1	0.50	2.21	9.2	3.1
CuNa-Beta	18.1	0.61	2.52	16.2	4.8
CuNa-Beta	18.1	0.66	2.93	14.2	3.6
CuNa-Beta	18.1	0.69	2.91	15.7	4.0
CuNa-Beta	18.1	0.69	2.59	12.7	3.7
CuNa-Beta	18.1	0.78	3.33	21.8	4.9
CuNa-Beta	18.1	0.88	3.17	18.4	4.4
CuNa-Beta	18.1	0.89	3.81	18.3	3.6
CuNa-Beta	18.1	0.90	3.88	20.3	3.9
CuNa-Beta	18.1	1.27	5.51	23.0	3.1
$CuNH_4$-Beta	20.0	0.28	1.12	4.8	3.2
$CuNH_4$-Beta	20.0	0.37	1.52	7.2	3.5
$CuNH_4$-Beta	20.0	0.60	2.37	15.1	4.8
$CuNH_4$-Beta	20.0	1.50	5.72	20.5	2.7
CuNa-Beta	42.0	0.17	0.38	0.0	0.0
CuNa-Beta	42.0	0.93	1.87	4.4	1.8
CuNa-Beta	42.0	2.15	4.14	12.6	2.3
CuNa-Beta	42.0	1.17	2.03	13.1	4.8
CuNa-Beta	42.0	1.74	3.66	15.4	3.2

presence of the $(Cu^{2+}X^{-}(H_2O)_5)^{+}$ complexes (17). Such type of "monovalent" Cu complexes were suggested to be ion exchanged adjacent to a single framework aluminum atom (17).

Figure 5 shows the effect of Cu loading on the position of the inflection point of the high-energy edge of the broad band of Cu-Beta zeolites. With increasing Cu loading for CuNa-Beta with Si/Al of 18.1, the high-energy edge of this broad band was shifted to higher wavenumbers and was proportional to Cu concentration in the zeolite. It reached a maximum value of ca. 15,800 cm^{-1} for Cu/Al ca. 1.3. By plotting wavenumbers of the inflection points of the broad band for all CoNa-Beta zeolites regardless of their Si/Al ratio vs Cu/Al values, the position of the inflection point increases again up to 15,800 cm^{-1} with increasing Cu/Al with leveling off at Cu/Al 1.3. This indicates the increasing exchange of monovalent $(Cu^{2+}X^{-}(H_2O)_5)^{+}$ complexes with Cu loading, and thus, incorporation of Cu ions complexes suggested to be balanced by one framework aluminum.

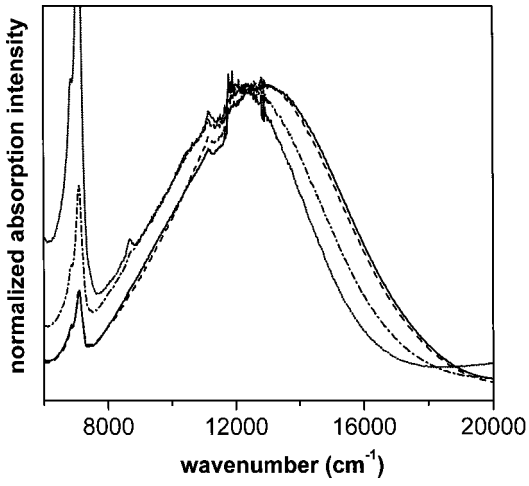

FIG. 4. Normalized vis–NIR DR spectra of as prepared Cu-Beta zeolites. Cu/Al 0.22, Si/Al 18.1 (●●●); Cu/Al 0.69, Si/Al 18.1 (- · · · -); Cu/Al 1.27, Si/Al 18.1 (- - -) and Cu/Al 2.15, Si/Al 42 (—).

Decomposition of NO over Cu-Beta Zeolites

Parent H- and Na-Beta zeolites were not active in NO decomposition, indicating that the Al-Lewis sites did not take part in the reaction. Conversion of NO to nitrogen over all the CuNa-Beta zeolites reached a constant value regardless of the zeolite pretreatment in various atmospheres. Time-on-stream (TOS) tests performed for 3 days showed stable activity of Cu-Beta zeolites in time. After activation of CuNa-Beta in a flow of helium at 720 K (see Fig. 6), a sharp increase in NO consumption was observed followed by a leveling off at a much lower value. On the other hand, after zeolite activation in a flow of oxygen, a slow increase in NO conversion was observed with TOS before a constant value was reached (see Fig. 6). Analogous behavior

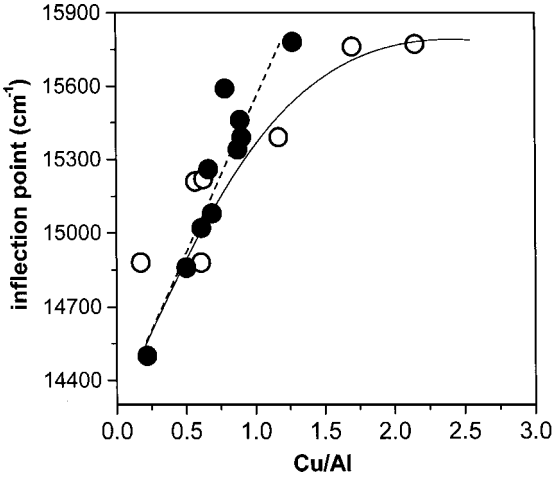

FIG. 5. The effect of Cu/Al on the position of high-energy inflection point of Cu^{2+} absorption band of as prepared Cu-Beta zeolites. All CuNa-Beta zeolites (○, —); CuNa-Beta zeolite, Si/Al 18.1 (●, - - -).

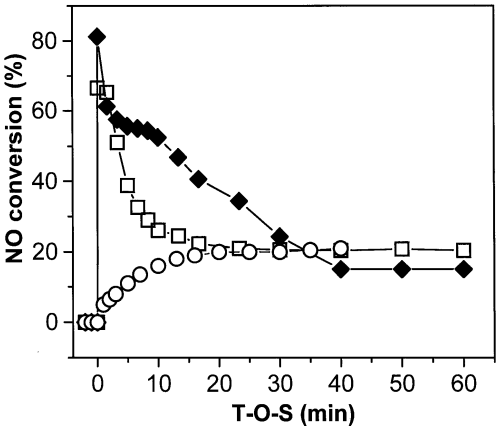

FIG. 6. The dependence of the decrease of NO concentration in reactor outlet on the reaction TOS. CuNa-Beta, Si/Al 18.1, Cu/Al 0.50, activation in He (□); $CuNH_4$-Beta, Si/Al 16.9, Cu/Al 0.56, activation in He (◆); CuNa-Beta, Si/Al 18.1, Cu/Al 0.50 activation in O_2 (○).

was observed by Ciambelli *et al.* (37) for Cu-ZSM-5 zeolites. It implies that the active site for NO decomposition is a copper in a monovalent state.

However, with CuH-Beta zeolites with Cu/Al < 0.6 pretreated in He, the leveling off of NO conversion occurred in two steps, as is shown in Fig. 6. At high Cu loadings (Cu/Al > 0.6), the behavior of CuH-zeolites in NO decomposition was similar to that of CuNa-Beta catalysts; a sharp decrease of NO conversion in the initial period was observed.

Vis–NIR spectra of the as-received CuNa-Beta zeolites are compared with the samples rehydrated after the catalytic test in Fig. 7. The Cu-zeolites with Cu loadings up to Cu/Al 0.5 exhibited after the catalytic reaction the Cu^{2+} spectra similar to the original as-received samples (Fig. 7a). On the contrary, the CuNa-Beta zeolites with high Cu loading (Cu/Al 1.3) became brown and their spectra were substantially changed (Fig. 7b). The intensity of the characteristic band of the Cu^{2+} ion around 12,000 cm^{-1} decreased and an intense absorption edge at ca. 20,000 cm^{-1} appeared. The edge of this absorption is similar to that of Cu_2O, but far from the absorption edge of CuO located in the NIR region (38). This indicates formation of some Cu_2O species during the catalytic reaction from the exchanged Cu^{2+} ions in the highly loaded Cu-Beta zeolites.

A dependence of catalytic activity of Cu-Beta zeolites on temperature exhibited a flat maximum ranging from 630 to 660 K. These maximum values of NO conversion were used in evaluation of the activity of various Cu-Beta zeolites with various Cu/Al/Si compositions. The highest NO conversion values (at the flat maximum) reached for the Cu-Beta zeolite with a given Si/Al ratio and corresponding TOF values (per Cu ion) are summarized in Table 2. These NO conversion values obtained per 400 mg of a zeolite and the TOF values (per "mean" Cu ion site) observed for Cu-Beta zeolites of various Cu/Al/Si compositions reached 70 and 50%, respectively, of the values reported by us at similar conditions for Cu-ZSM-5.

As follows from Table 2, the NO conversion over Cu-Beta with different Si/Al was not proportional to the Cu concentration and also the dependence of TOF on Cu/Al did not show any correlation. This indicates the presence of several Cu species with different activity in NO decomposition and their different distribution in the Beta zeolites. Moreover, the variation of the TOF values indicates that more than one parameter controls the distribution of the active Cu species in the Beta zeolites.

The dependence of TOF on Cu loading in Cu-Beta zeolites of various compositions is shown in Fig. 8. For CuNa-Beta zeolites (Figure 8a), conversion of NO was not observed at low Cu loading (Cu/Al < 0.25). At medium Cu loadings (Cu/Al ca. 0.25–1.0), the TOF sharply increased with Cu loading and passed a maximum, which was observed at higher Cu/Al values for a zeolite with a higher Si/Al ratio equal to 42. On the other hand, the Cu ions in CuH-Beta, prepared from the parent NH_4-Beta (Fig. 7b), exhibited high TOF values already at low Cu loadings (Cu/Al < 0.25), with the maximum TOF value reached at a Cu/Al concentration lower lower than that for CuNa-Beta zeolites. It is important to note that the maxima in TOF values for both CuNa- and CuH-Beta zeolites were shifted to

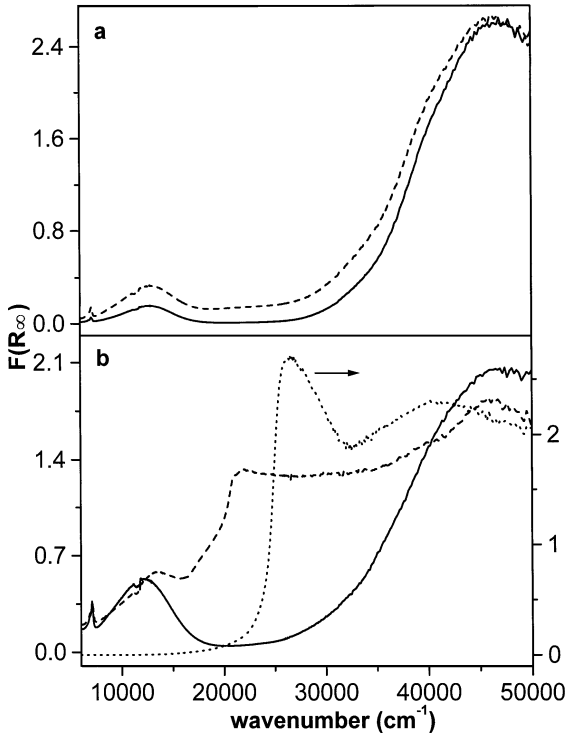

FIG. 7. The effect of reaction run followed by rehydration on the spectra of CuNa-Beta (Si/Al 18.1). (a) Cu/Al 0.50, as-prepared (—); after reaction run (- - - -). (b) Cu/Al 1.27, as-prepared (—), after reaction run (- - - - -), bulk Cu_2O (●●●●●●).

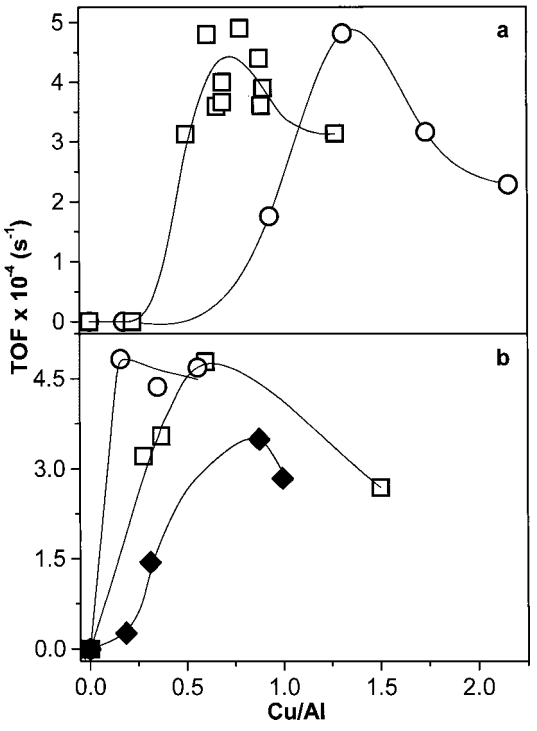

FIG. 8. The effect of Cu loading on TOF in NO decomposition over (a) CuNa-Beta zeolite, Si/Al 18.1 (□); Si/Al 42 (○). (b) $CuNH_4$-Beta zeolite, Si/Al 16.9 (○); $CuNH_4$-Beta zeolite, Si/Al 20 (□); and CuH-Beta zeolite, Si/Al 14.3 (◆).

higher Cu/Al concentrations with higher Si/Al ratios. The behavior of CuH-Beta zeolite prepared from the H-Beta zeolite, with respect to increase of NO conversion at low Cu/Al loadings, was between that of CuNa- and that of $CuNH_4$-Beta catalysts (Fig. 8b).

The highest values of TOF reached for zeolites with similar Si/Al ratios, but regardless of Cu concentration, i.e., for zeolites with the Cu ions exhibiting the highest activity, have been used for estimation of the effect of Si/Al composition on the Cu ion activity in NO decomposition. This dependence is depicted in Fig. 9. For the range of Si/Al 12–17, the TOF values sharply increased with decreasing concentration of aluminum in the framework, but at Si/Al values above 17 the TOF values seem to be independent of the aluminum concentration.

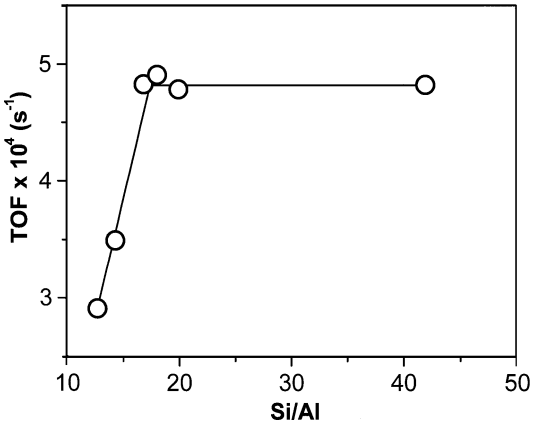

FIG. 9. The effect of Si/Al on the maximum TOF values found with Cu-Beta (see Table 2).

DISCUSSION

Under the same reaction conditions conversions of NO ranging from 5 to 24% and TOF values from 0.2 to $0.5 \times 10^{-3}\,s^{-1}$ over Cu-Beta zeolites, depending on Cu/Si/Al composition, are in the same order as those for Cu-ZSM-5 zeolites at 10–34% of NO conversion and TOF of $0.2–1.7 \times 10^{-3}\,s^{-1}$ (cf. Table 2). This indicates, that the well-known high and stable catalytic activity in NO decomposition of the Cu ions exchanged in ZSM-5 (3, 5) is not unique for the ions implanted in the ZSM-5 matrix and is general for the Cu ions exchanged in matrices exhibiting low local negative framework charge, like silicon-rich zeolites. This suggestion is supported by recent observations of catalytic activity in NO decomposition of the Cu ions Cu–*Me*APO molecular sieves (27–29), where the framework local negative charge density $((Al + P)/Me^{2+})$ can be expected to be similar to that existing in silicon-rich zeolites.

Similarity between Cu-Beta zeolite (cf. Fig. 6) and Cu-ZSM-5 (37) in the transient behavior of NO decomposition after activation in helium and opposite behavior after activation in oxygen evidenced that monovalent Cu species, like that suggested for Cu-ZSM-5 (37, 39), represent the active center for NO decomposition over Cu-Beta catalysts. Moreover, the framework of Beta topology contains local arrangements similar to those suggested to form the Cu sites in ZSM-5 zeolite (cf. Refs. 18, 40, 41 and Fig. 10). Also, characteristic emission spectra of the individual Cu^{2+} ions and the characteristic IR bands of NO adsorbed onto Cu^{2+} in Beta zeolites of various Cu/Al/Si compositions (42, 43) are similar to those reported for Cu^{+}-ZSM-5 (15, 16, 18). It indicates that similar Cu^{+} species might represent the active center for NO decomposition over Cu-Beta and Cu-ZSM-5 zeolites.

The dependence of TOF on Cu loading of CuNa-Beta zeolites, shown in Fig. 8a, shows the presence of three different Cu species, denoted here as Cu-1, Cu-2, and Cu-3. It can be suggested that the Cu-1 species is formed in CuNa-Beta zeolite at low Cu loading (Cu/Al < ca. 0.25) and it is not active in NO decomposition. The Cu-2 species is formed at medium Cu loading (Cu/Al ca. 0.25–1.0), and it represents the Cu site responsible for NO decomposition. The Cu-3 species is formed at high Cu loading (Cu/Al ca. > 1) and is also inactive in NO decomposition, or exhibits much lower activity compared to the Cu-2 species. As follows from VIS spectra of the hydrated Cu-Beta zeolites after the reaction

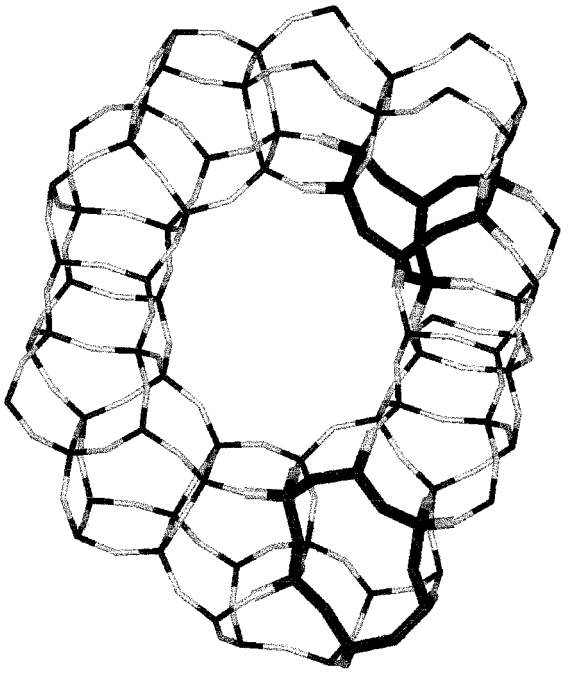

FIG. 10. Framework structure of Beta zeolite. Structure according to Ref. (41).

run (cf. Fig. 7), the Cu-1 and Cu-2 species represent single Cu ions. After rehydration, these Cu ions exhibit spectra similar to those of the Cu ions in the original, nontreated, zeolite samples. The Cu-3 species represents noncationic Cu species formed during the reaction in Cu-Beta with Cu/Al loading about 1.0 (but not below 0.5). This is evidenced by a significant decrease of the absorption intensity of the single Cu^{2+} ions at 12,000–13,000 cm^{-1} after the reaction run and rehydration, as is shown in Fig. 7b. This decrease of concentration of single Cu^{2+} ions in zeolite is accompanied by an appearance of a new, strong absorption edge at ca. 19,000 cm^{-1}. This position of the absorption edge excludes identification of the Cu-3 species as CuO exhibiting absorption edge in NIR region (38), but it is close to the characteristic edge of Cu_2O (is also shown in Fig. 7b). The shift of 2000 cm^{-1} of the absorption edge of the Cu-3 moiety to higher wavenumbers compared to the bulk Cu_2O (17,000 cm^{-1}) indicates that it does not represent bulky Cu_2O oxide, but some small Cu_2O particles.

A shift of the Cu^{2+} absorption band of the exchanged Cu^{2+} (see Fig. 4) reflects presence of Cu^{2+} with different ligands in Cu-Beta zeolites (see Results). The shift to the higher wavenumbers indicates increasing concentration of the hydrated Cu^{2+} ions balanced by a single framework aluminum atom (17). The concentration of this type of Cu complexes increased with Cu/Al, as is shown in Fig. 5. For the CuNa-Beta zeolite (Cu/Al 0.22, Si/Al 42) nonactive in NO decomposition, the lowest value of the absorption edge of the Cu^{2+} band (14,500 cm^{-1}) was observed. This value is close to the position of the absorption edge of the Cu^{2+} hexaaquocomplex in aqueous solution of $CuCl_2$, which is 14,300 cm^{-1} (17). For comparison, the Cu^{2+} edge in Cu acetate solution, where the presence also of a $(Cu^{2+}–X^{-}(H_2O)_5)^{+}$ complex can be expected, is ca. 15,400 cm^{-1}.

Thus, the Cu-1 species, inactive in NO decomposition, represents the Cu exchanged as divalent $(Cu^{2+}(H_2O)_6)^{2+}$ ions, which are balanced by two close framework aluminum atoms. The shift of the absorption edge of CuNa-Beta increasing with Cu/Al loading is followed by an increase of TOF values per Cu ion in NO decomposition (Fig. 11). Saturation of the increase in TOF values at high Cu/Al concentration and then following decrease of catalytic activity with the edge shift observed for the highest edge positions, i.e., for the highest Cu loading, can be explained by the formation of inactive or very low active Cu-3 species. These species are evidenced in the Vis-NIR spectra after the reaction run (not shown in the figures). It can be seen that the Cu-2 species represents the Cu ions balanced by a single framework aluminum atom, and Cu-1 species represents the Cu ions located in the vicinity of two close aluminum atoms.

The attribution of the inactive Cu-1 species to the Cu ions balanced by two aluminum atoms and of the Cu-2 species to those balanced by a single aluminum is supported by the maximum TOF values observed for the dependence of TOF on Si/Al ratio. With increasing Si/Al ratio from 12 to 17, a decrease in the presence of close framework aluminum atoms, making it possible to balance divalent cations, can be assumed, according to the statistical study on Al distribution in ZSM-5 (44). Thus, a relative concentration of Cu ions balanced by a single aluminum increases with Si/Al and is followed by an increase in the catalytic activity related to one Cu ion (TOF), as is documented in Fig. 11. At low aluminum content in the zeolite (ca. Si/Al $\geq$ 20), the probability of the presence of close aluminum atoms can

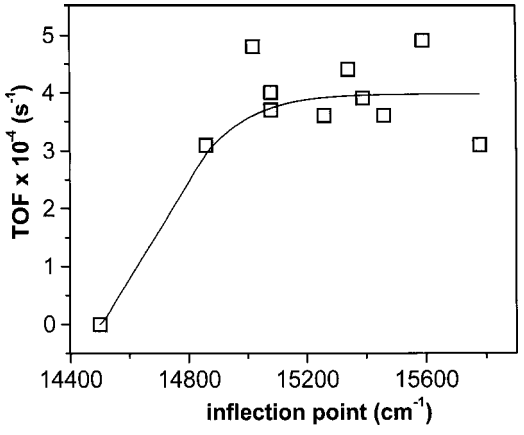

FIG. 11. The relation between the position of high-energy inflection point of Cu^{2+} absorption band of as-prepared CuNa-Beta zeolite (Si/Al 18.1) and their TOF in NO decomposition.

be assumed to be low and the presence of Cu ions balanced by single aluminium can be expected. This assumption is confirmed by the saturation of TOF values for this range of Si/Al ratios (>17).

A comparison of the activity of the Cu ions depending on the concentration of Cu in the zeolites, on TOS, and on the type of Na-, NH_4-, and H-parent Beta into which the Cu ions were incorporated provides additional information on the effect of framework aluminum on the character of bonding and reactivity of Cu ions in Beta zeolites. The Cu ions in CuH-Beta zeolites prepared from the parent NH_4-Beta zeolites exhibited higher catalytic activity at low Cu loadings than those in CuNa-Beta zeolites (see Fig. 8). The behavior of both CuH- and $CuNH_4$-Beta zeolites of low and medium Cu loading (Cu/Al < 0.5) at low TOS of the decomposition reaction differed from that of CuNa zeolites. Leveling of the NO conversion required much a longer time (ca. twice), and it exhibited two steps in dependence on TOS (see Fig. 6). Because the zeolite deammination occurred during its activation procedure and, moreover, these two steps in conversion depending on TOS were observed for both CuH zeolites, the behavior during the initial reaction period should reflect the redistribution of the Cu ions under the reaction performance. It can be expected that most of the Cu ions in $CuNH_4$-Beta zeolites were originally adjacent to one aluminum atom, but some of them migrated under the reaction conditions to sites in the vicinity of two aluminum atoms. The Cu ion migration was reflected in two or three time higher activity in the first 20 min of the decomposition reaction (see Fig. 6). On the other hand, the Cu ions in CuNa-Beta were exchanged at low loading in the vicinity of two aluminum atoms (see Fig. 4). Migration of a substantial part of the Cu ions to sites in the vicinity of one Al atom under the reaction was impossible because these sites were occupied by Na ions. CuH-Beta prepared from the protonized form of parent zeolite exhibited significantly lower activity both in the final stage and in the initial period. This reflects a higher probability of the presence of divalent Cu complexes under more acidic conditions of ion exchange (cf. Ref. 17) into the H-Beta zeolite, followed by preferential exchange of Cu ions in the vicinity of two aluminum atoms. At high Cu loading, the differences in catalytic activity between CuNa- and CuH-Beta zeolites are not significant. At high Cu loading, the migration of Cu ions is restricted due to the occupation of the majority of cationic sites by the Cu ions.

A very important feature, typical of Beta structure, is a significant concentration of Lewis sites in H-Beta zeolites. These Lewis sites result from distortions of the Beta framework (34, 35, 45). Lewis sites are still present in CuH-Beta zeolites at low Cu loading prepared from parent NH_4 zeolite. On the other hand, in CuNa-Beta zeolites prepared from parent sodium from a zeolite, the Lewis sites are not present (see Fig. 3). Because similar maximum TOF values were observed for CuH-Beta at low Cu loading and CuNa-Beta with complete loading by Cu ions (4.8 and 4.8–4.9×10^{-4} s^{-1}, resp.), defects of structure and a presence of Lewis sites do not affect the activity of Cu ions in NO decomposition.

Knowledge of the distribution of active and inactive Cu species in Cu-Beta, together with that of their redistribution during the initial period of the NO decomposition, enables the estimation of the activity of Cu-2 species in NO decomposition. Catalytic activity of the Cu-2 species in low-loaded $CuNH_4$-Beta zeolites can be assumed to be close to the plateau on the TOS dependence, depicted in Fig. 6. Under this presumption, TOF = $1.5–2.0 \times 10^{-3}$ s^{-1} corresponds to the Cu-2 species in CuH-Beta. Estimation of the TOF value of the Cu-2 species in CuNa-Beta zeolite is more uncertain. For CuNa-Beta with an Si/Al ratio around 18.1, only inactive Cu-1 ions are exchanged to the Cu/Al level 0.25–0.3 (see Fig. 8a). At Cu loadings higher than Cu/Al 0.5, formation of inactive Cu-3 species occurs and estimation of the concentration of this species is difficult. Taking into account very rough estimation of the concentration of Cu-1 and Cu-3 species from a graph on Fig. 8a, a TOF value of 1.0–1.9×10^{-3} s^{-1} corresponds to the Cu-2 species of CuNa-Beta zeolite. The highest TOF value was reported for Cu-ZSM-5 with 85% of active Cu species in zeolite (14, 16), reflected in 540-nm Cu^+ emission. This content of active Cu in ZSM-5, under the reaction conditions applied on Cu catalysts in this work, corresponds to TOF = 2×10^{-3} s^{-1}. It can be concluded that the catalytic activities of the Cu species active in NO decomposition in ZSM-5 and Beta zeolite matrices are similar.

The catalytic behavior of Cu-Beta and identification of three Cu species formed under reaction conditions of NO decomposition in Cu-Beta zeolites are similar to those reported for Cu-ZSM-5, but trends observed in catalytic behavior and Cu distribution are more pronounced for Cu-Beta zeolites. An approximately sigmoidal dependence of TOF on Cu/Al loading, an increase of catalytic activity of Cu ions with decrease of framework aluminum content, the presence of two types of Cu^+ ions (one inactive) in catalysts, an effect of Al distribution on the distribution of Cu ions, and the formation of inactive oxidic species at high Cu loading were reported (3, 14–17, 38, 46). Attribution of the catalytic activity of Cu-Beta zeolites to single Cu^+ ions is in agreement with the suggestion that the single Cu^+ ions or adjacent Cu^{2+} and O^- centers act as catalytic sites in Cu-ZSM-5 (3–18). This is supported mainly by the similarity of vis–NIR spectra of the fresh sample and the sample exhibiting the highest TOF value after the reaction. This finding also excludes the possibility that Cu oxidic species serve as active centers. Attribution of the active Cu-2 ions to the Cu species and high activity of the Cu ions exchanged in zeolites with Si/Al > 40 indicate that close Cu^+ ions are not the most active sites for NO decomposition (3–18). Due to the

low aluminum content and large cavities on the channels crossings of Beta zeolite (diameter ca. 9 Å), the distance between neighboring Cu ions is rather high, approximately 6 Å according to the computed model (BEA structure according to Ref. 41). The Cu–O distance is assumed to be 2 Å as followed from EXAFS investigations of the Cu ions in zeolite (11, 12). Cations are assumed to be coordinated to six-member rings, similar to that seen in the Co ions (19). For Si/Al > 40, an even larger distance between Cu ions must be assumed. A maximum Cu–Cu distance for Cu^+–Cu^+ pairs equal to 4 Å was suggested according to an EXAFS experiment (47). A maximum Cu–Cu distance of 2.9 Å corresponds to that seen in Cu^{2+}–O–Cu^{2+} species (Cu^{2+} diameter 0.7, oxygen diameter 1.4 Å). Moreover, the presence of close Cu ions in highly active CuH-Beta samples with Cu/Al ratio 0.16 and Si/Al 20 (i.e., with one Cu ion per 125 framework T atoms) can hardly be accepted. This is in agreement with the observation of Kucherov *et al.* (48) for Cu-ZSM-5, where, according to EPR, the formation of aggregated species is of minor importance. It is necessary to note that the above-mentioned spectroscopic studies have usually been carried out on samples with unknown catalytic activity and without knowledge of the concentration of the individual Cu species.

Thus, catalytic centers in Cu-loaded high silica zeolites represents single Cu^+ ions, probably with adjacent O centers or extra-lattice-oxygen species on single Cu ions. This suggestion is also supported by the effect of framework charge density on NO decomposition over Cu-CHAB molecular sieves (29). A decrease of framework charge density (from Si/Al 2.7 of chabazite to (P + Al)/Zn 9 of ZnAlPO-34—topology identical to that of (CHAB) was followed by the appearance of catalytic activity, while Cu-chabazite was completely inactive.

CONCLUSIONS

Cu ions in Beta zeolites exhibit high and stable catalytic activity in NO decomposition which is comparable to that of the Cu ions located in ZSM-5. Three Cu-type species were identified in Cu-Beta catalysts:

The Cu-1 species represent Cu ions balanced by two close framework aluminum atoms. These Cu ions are inactive in NO decomposition and are preferentially exchanged into Na-Beta zeolite.

The Cu-2 species are responsible for the catalytic activity of Cu-Beta zeolite in NO decomposition. They are suggested to be the single Cu ions balanced by a one-framework aluminum atom. These Cu ions are exchanged into Na-Beta zeolite at medium Cu loading and to NH_4-Beta also at low Cu loading.

The Cu-3 species are Cu ions in Cu_2O in a form of small clusters. These Cu_2O dispersed particles are formed during the reaction and reach high concentration at high Cu loading in the zeolite. However, their catalytic activity in NO decomposition is negligible.

ACKNOWLEDGMENTS

This work was supported by the Academy of Sciences of the Czech Republic under Project S4040016. Additional financial support for this research from Unipetrol a.s. is highly acknowledged. The authors thank to Dr. T. Grygar for the chemical analysis of zeolites.

REFERENCES

1. Iwamoto, M., Yahiro, H., Tanda, K., Mizuno, N., and Mine, Y., *J. Phys. Chem.* **95**, 3727 (1991).
2. Iwamoto, M., and Yahiro, H., *Catal. Today* **22**, 5 (1994).
3. Liu, D.-J., and Robota, H. J., *Catal. Lett.* **21**, 291 (1993).
4. Schneider, W. F., Haas, K. C., Ramprasad, R., and Adams, J. B., *J. Phys. Chem.* **100**, 6032 (1996).
5. Haas, K. C., and Schneider, W. F., *J. Phys. Chem.* **100**, 9292 (1996).
6. Ramprasad, R., Schneider, W. F., Haas, K. C., and Adams, J. B., *J. Phys. Chem. B* **101**, 1940 (1997).
7. Yokomichi, Y., Yamabe, T., Otsuka, H., and Kakumoto, T., *J. Phys. Chem.* **100**, 14424 (1996).
8. Blint, R. J., *J. Phys. Chem.* **100**, 19518 (1996).
9. Trout, B. L., Chakraborty, A. K., and Bell A. T., *J. Phys. Chem.* **100**, 4173 (1996).
10. Trout, B. L., Chakraborty, A. K., and Bell A. T., *J. Phys. Chem.* **100**, 17582 (1996).
11. Spoto, G., Zecchina, A., Bordiga, S., Ricchiardi, G., Martra, G., Leofanti, G., and Petrini, G., *Appl. Catal. B* **3**, 151 (1994).
12. Anpo, M., Matsuoka, M., Shioya, Y., Yamashita, H., Giamello, E., Morterra, C., Che, M., Patterson, H. H., Weber, S., Oullette S., and Fox, M. A., *J. Phys. Chem.* **98**, 5744 (1994).
13. Teraishi, K., Ishida, M., Irisawa, J., Kume, M., Takahashi, Y., Nakano, T., Nakamura, H., and Miyamoto, A., *J. Phys. Chem. B* **101**, 8079 (1997).
14. Wichterlová, B., Dědeček, J., and Vondrová, A., *J. Phys. Chem.* **99**, 1065 (1995).
15. Dědeček, J., Sobalík, Z., Tvarůžková, Z., Kaucký, D., and Wichterlová, B., *J. Phys. Chem.* **99**, 16327 (1995).
16. Wichterlová, B., Dědeček, J., Sobalík, Z., Vondrová, A., and Klier K., *J. Catal.* **169**, 194 (1997).
17. Dědeček, J., and Wichterlová, B., *J. Phys. Chem. B* **101**, 10233 (1997).
18. Dědeček, J., and Wichterlová, B., *Chem. Phys. Phys. Chem. B* **1**, 629 (1999).
19. Kaucký, D., Dědeček, J., and Wichterlová, B., *Microp. Mesopor. Mater.* **31**, 75 (1999).
20. Liu, D.-J., and Robota, H. J., *Appl. Catal. B* **4**, 155 (1994).
21. Jang, H.-J., Hall, W. K., and d'Itri, J., *J. Phys. Chem.* **100**, 9416 (1996).
22. Valyon, J., and Hall, W. K., *J. Phys. Chem.* **97**, 7054 (1993).
23. Valyon, J., and Hall, W. K., *J. Catal.* **143**, 520 (1993).
24. Sarkany, J., d'Itri, J., and Sachtler,W. M. H., *Catal. Lett.* **16**, 241 (1992).
25. Lei, G. D., Adelman, B. J., Sarkany, J., and Sachtler W. M. H., *Appl. Catal. B* **5**, 245 (1995).
26. Larsen, S. C., Aylor, A. W., Bell, A. T., and Reimer, J. A., *J. Phys. Chem.* **98**, 11533 (1994).
27. Dědeček, J., Čejka, J., and Wichterlová, B., *Appl. Catal. B* **15**, 233 (1998).
28. Dědeček, J., Vondrová, A., and Čejka, J., *Collect. Czech Chem. Commun.* **63**, 1755 (1998).

29. Dědeček, J., Vondrová, A., and Čejka, J., *Collect. Czech Chem. Commun.* **65**, 343 (2000).
30. Rubin, M. K., U.S. patent 5, 164 169 (1992).
31. Eapen, M. J., Reddy, K. S. N., and Shiralkar, V. P., *Zeolites* **14**, 295 (1994).
32. Kortüm, G., "Reflexionsspektroskopie," Springer-Verlag, Berlin 1969.
33. Wichterlová, B., Tvarůžková, Z., Sobalík, Z., and Sarv, P., *Microporous Mesoporous Mater.* **24**, 223 (1998).
34. Bourgeat-Lami, E., Massiani, P., Di Renzo, F., Espiau, P., and Fajula, F., *Appl. Catal.* **72**, 139 (1991).
35. Kiricsi, I., Flego, C., Pazzuconi, G., Parker, W. O., Jr., Millini, R., Perego, C., and Bellussi, G., *J. Phys. Chem.* **98**, 4627 (1994).
36. Bortnovsky, O., Sobalík, Z., and Wichterlová, B., submitted.
37. Pirone, R., Ciambelli, P., Moretti, G., and Russo, G., *Catal. Lett.* **430**, 255 (1997).
38. Dědeček, J., Ph.D. thesis, J. Heyrovský Institute of Physical Chemistry, Prague, 1995.
39. Iwamoto, M., and Hamada, H., *Catal. Today* **10**, 57 (1991).
40. Dědeček, J., Kaucký, D., and Wichterlová, B., *Microporous Mesoporous Mater.* **35–36**, 483 (2000).
41. Newsam, J. M., Treacy, M. M. J., Koetsier, W. T., and de Gruyter, C. B., *Proc. R. Soc. (London) A* **420**, 375 (1988).
42. Canonico, F., Diploma thesis, Iniversita' degli studi di Torino, Torino, 1999.
43. Canonico, F., Zecchina, A., Dědeček, J., and Wichterlová, B., unpublished results.
44. Rice, M. J., Chakraborty, A. K., and Bell, A. T., *J. Catal.* **186**, 222 (1999).
45. Vimont, A., Thibault-Starzyk, F., and Lavalley, J. C., *J. Phys. Chem. B* **104**, 286 (2000).
46. Millar, G. J., Canning, A., Rose, G., Wood, B., Trewartha, L., and Mackinnon, I. D. R., *J. Catal.* **183**, 169 (1999).
47. Kuroda, Y., Kumashiro, R., Yoshimoto, T., and Nagao, M., *Phys. Chem. Chem. Phys.* **1**, 649 (1999).
48. Kucherov, A. V., Shigapov, A. N., Ivanov, A. A., and Shelef, M., *J.Catal.* **186**, 334 (1999).